AD_____

Award Number: DAMD17-02-1-0106

TITLE: Non-Invasive Diagnosis of Androgen Sensitivity in Human Prostate Tumors

PRINCIPAL INVESTIGATOR: Laurel O. Sillerud, Ph.D.

CONTRACTING ORGANIZATION: University of New Mexico Health Science Center
Albuquerque, New Mexico 87131-5041

REPORT DATE: February 2003

TYPE OF REPORT: Annual

PREPARED FOR: U.S. Army Medical Research and Materiel Command
Fort Detrick, Maryland 21702-5012

DISTRIBUTION STATEMENT: Approved for Public Release;
Distribution Unlimited

The views, opinions and/or findings contained in this report are those of the author(s) and should not be construed as an official Department of the Army position, policy or decision unless so designated by other documentation.

20030602 066

REPORT DOCUMENTATION PAGE

Form Approved
OMB No. 074-0188

Public reporting burden for this collection of information is estimated to average 1 hour per response, including the time for reviewing instructions, searching existing data sources, gathering and maintaining the data needed, and completing and reviewing this collection of information. Send comments regarding this burden estimate or any other aspect of this collection of information, including suggestions for reducing this burden to Washington Headquarters Services, Directorate for Information Operations and Reports, 1215 Jefferson Davis Highway, Suite 1204, Arlington, VA 22202-4302, and to the Office of Management and Budget, Paperwork Reduction Project (0704-0188), Washington, DC 20503

1. AGENCY USE ONLY (Leave blank)	2. REPORT DATE	3. REPORT TYPE AND DATES COVERED
	February 2003	Annual (15 Jan 02 - 14 Jan 03)

4. TITLE AND SUBTITLE
Non-Invasive Diagnosis of Androgen Sensitivity in Human Prostate Tumors

5. FUNDING NUMBERS
DAMD17-02-1-0106

6. AUTHOR(S) :
Laurel O. Sillerud, Ph.D.

7. PERFORMING ORGANIZATION NAME(S) AND ADDRESS(ES)
University of New Mexico Health Science Center
Albuquerque, New Mexico 87131-5041

E-Mail: laurel@unm.edu

8. PERFORMING ORGANIZATION REPORT NUMBER

9. SPONSORING / MONITORING AGENCY NAME(S) AND ADDRESS(ES)
U.S. Army Medical Research and Materiel Command
Fort Detrick, Maryland 21702-5012

10. SPONSORING / MONITORING AGENCY REPORT NUMBER

11. SUPPLEMENTARY NOTES
Original contains color plates: All DTIC reproductions will be in black and white.

12a. DISTRIBUTION / AVAILABILITY STATEMENT
Approved for Public Release; Distribution Unlimited

12b. DISTRIBUTION CODE

13. Abstract ***(Maximum 200 Words)*** *(abstract should contain no proprietary or confidential information)*

We characterized human prostate tumors by histology and quantitative NMR spectroscopy to determine if altered prostate gene expression produced NMR detectable changes in several metabolites (e.g., citrate, triacylglycerols, taurine, tyrosine). These may provide sensitive and specific predictors of the presence, and the androgen sensitivity, of prostatic adenocarcinoma. Our investigations provided a sound biochemical basis for the application of non invasive, *in vivo* NMR spectroscopy to assess tumor differentiation and androgen sensitivity in prostate cancer patients. We established a conventional tissue diagnosis by optical histology and computer-aided measurement of epithelial area, on the NMR tissue samples, assigned a Gleason score to each sample, and performed *in vitro* quantitative ^{1}H and ^{13}C NMR spectroscopic measurements of the metabolic markers on tissue samples from human prostate tumors and adjacent non tumor tissue. Computer based Linear Discriminant Analysis will be used to develop a discrimination function based on the NMR spectroscopic measurements, the histology, Gleason score, and PSA measurements, and the patient's progress, to determine the most specific and sensitive NMR spectroscopic predictors of tumor diagnosis, grade, and hormonal sensitivity. We then applied NMR spectroscopy to human patients to measure the metabolites determined above as the most sensitive and specific predictors of grade, stage and hormonal responsiveness, and will compare the measurements with patient outcomes.

14. SUBJECT TERMS:	15. NUMBER OF PAGES
prostate cancer	17
	16. PRICE CODE

17. SECURITY CLASSIFICATION OF REPORT	18. SECURITY CLASSIFICATION OF THIS PAGE	19. SECURITY CLASSIFICATION OF ABSTRACT	20. LIMITATION OF ABSTRACT
Unclassified	Unclassified	Unclassified	Unlimited

Table of Contents

DOD Prostate cancer program Annual report.

Project Title: " Non-Invasive Diagnosis of Androgen Sensitivity in Human Prostate Tumors "

Principal Investigator: Laurel O. Sillerud, Ph.D.

Institution: *University of New Mexico School of Medicine,*
Department of Molecular Biology and Biochemistry,
Albuquerque, NM 87131

Introduction

Prostatic adenocarcinoma is expected to be diagnosed in more than 200,000 American men in 2003, leading to more than 40,000 deaths. In order to enhance the survival of these cancer patients new methods for tumor diagnosis and characterization are urgently required. This work seeks to develop a foundation for new methods for tumor characterization through quantitative, nuclear magnetic resonance (NMR) spectroscopy of prostate tissue *in vitro* and the human prostate *in vivo*. This research is particularly timely and important because the results can be rapidly transferred to other institutions due to the widespread availability of suitable clinical MRI instruments. The scientific basis for this research rests on the fact that the metabolism of the normal, highly-differentiated, prostate is unique among bodily tissues in that it maintains, and secretes, large amounts of intermediary compounds, like citrate. This normal metabolism is observable by means of NMR spectroscopy, both *in vitro* and *in vivo*. Tumorigenesis in the prostate occurs with dedifferentiation and profound metabolic changes which again are observable with NMR. Our preliminary results have shown that qualitative NMR spectroscopy can not only distinguish malignant from non-malignant prostate tissue, but that it can also answer the very important clinical question of whether or not a given prostate tumor is androgen sensitive. In particular, NMR detectable metabolites such as citrate, and triacylglycerols may serve to differentiate tumor from benign tissue, while taurine and tyrosine may serve as indicators of the androgen sensitivity of tumors. It remains to be determined, however, which quantitative NMR metabolite measurements provide the most specific and sensitive predictors of malignancy and androgen sensitivity in human prostatic tissue.

Body

We proposed a series of related histological, NMR spectroscopic, and computer-based analyses of human prostate tumor tissue *in vitro* and *in vivo*. Since this is the initial funding year, our primary focus has been on setting up and validating the technology needed to carry out these related tasks and on collecting tissue samples and patients for study.

A. Histology.

We have performed optical histology on surgical resections of human prostate tissue. The first emphasis was on the use of standard Hematoxylin and Eosin stains. . Prostatic adenocarcinomas are given a histologic grade (Gleason's grading system is used most often, and includes a score of 1 to 5 for the most prominent component added to a score of 1 to 5 for the next most common pattern). Figure 1 shows representative, low magnification views of H&E-stained sections of normal (left) and

Gleason grade 9 (right) human prostate tumors. The normal glandular architecture is visible on the left, with well-isolated acini embedded within dense stroma. The glandular lumens are clear and there is only moderate hypertrophy of the epithelial elements in a portion of the acini, with loss of intervening stroma. The adenocarcinoma sample on the right was given a Gleason grade of 4+5=9. The glandular lumens have been filled with neoplastic tumor cells in most cases, but some lumens have simply lost their epithelium and only retain their basement membrane. There is also infiltration of the stroma by tumor cells. We assigned a Gleason score to each tumor sample.

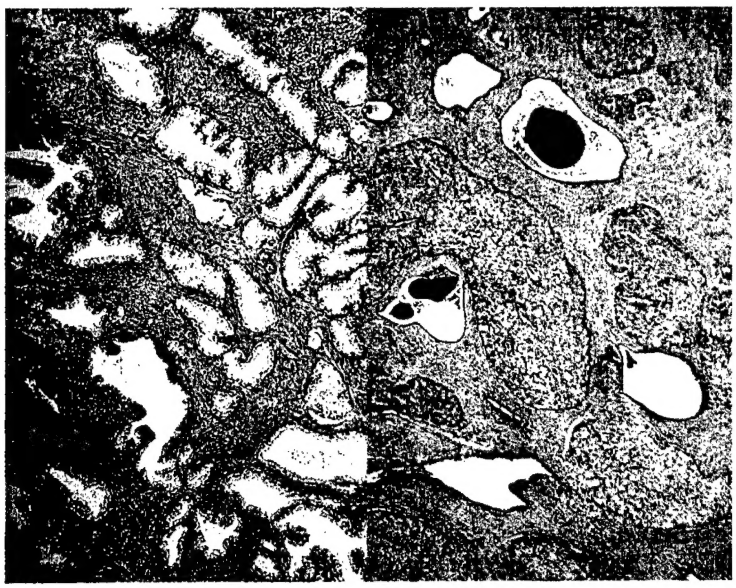

Figure 1. Hematoxylin and Eosin stained sections of human prostate tissue samples. Normal (left) and Gleason grade 9 (right) tumor tissues.

The normal histologic appearance of prostate glands and surrounding fibromuscular stroma is shown at high magnification in Fig. 2 (left). The normal prostate tissue on the left shows well-differentiated glands lined with tall columnar epithelial cells. The nuclei are located at the bases of the epithelial cells, next to the prominent basement membrane. These cells do not have prominent nucleoli or mitotic figures. On the right is prostatic adenocarcinoma. Note how the glands of the carcinoma are completely filled with tumor cells evidently derived from the epithelium. This tumor sample shows prominent nucleoli and mitotic figures. The stroma appears relatively normal, except for the areas of tumor invasion.

We used computer-aided measurements of epithelial area in these sections to derive values for the relative amounts of epithelium in normal and malignant samples. Normal prostate contains modest amounts of epithelium; the average is 12.7 ± 5.9 % by area. Prostatic adenocarcinoma, on the other hand contains twice the epithelium at 25.3 ± 7.9 % by area. This is a clear reflection of the fact that most prostatic adenocarcinoma cells have an epithelial origin.

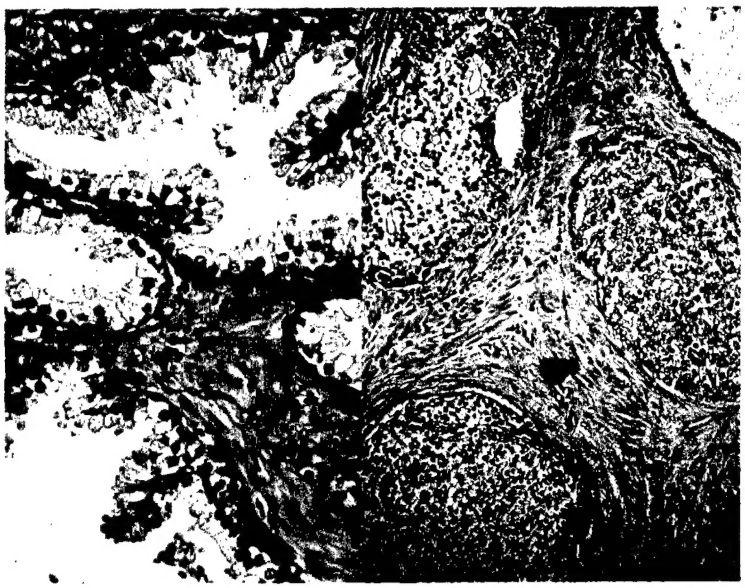

Figure 2. High-magnification photomicrographs of Hematoxylin and Eosin stained sections of human prostate adenocarcinoma samples. Normal (left) and Gleason grade 9 (right) tumor tissues.

Our next task will be to utilize special stains (Oil Red O, Prostate Specific Antigen, Prostatic Acid Phosphatase) to reveal additional tissue characteristics for adenocarcinoma compared with normal controls. Our hypothesis is that the increased lipids found in prostate adenocarcinoma samples will be observable with the aid of lipid-specific stains, such as Oil Red O. We also expect that the alteration in gene expression which results in tumorigenesis will lead to enhanced staining for Prostate Specific Antigen, and perhaps Prostatic Acid Phosphatase. We will develop antibody-based staining techniques (commercially available) for these antigens as well.

B. *In vitro* quantitative ^{13}C NMR spectroscopy.

Our task here was to develop quantitative one-dimensional ^{13}C NMR spectroscopy for the non-destructive measurement of metabolites in human tissue samples from resected prostates. This required us to perform calibration of the NMR standards and pulse sequences. As an example of the work performed along these lines, we use our calibration of the citrate ^{13}C NMR signals. The observation of metabolite signals in the NMR spectrum of a mixture is not necessarily quantitative unless attention is paid to several, well-known features of NMR spectroscopy. (1) The NMR signals are acquired using signal averaging in which multiple samplings of the free induction decay (FID) from the sample are coherently added in the spectrometer computer memory. These samplings are repeated as often as is practical (2-3 per second) in order to build up adequate signal to noise for the FID. The nuclear magnetization does not return to thermal equilibrium under these conditions because the NMR relaxation times are on the order of 1-2 seconds. Therefore, the NMR relaxation times must be measured and the data must then be corrected for this partial saturation of the NMR signals. Fortunately, this correction is easily measured and applied. For example, we measured the NMR relaxation time for the 2,5 carbons of citrate to be 1.6 seconds in physiological saline at pH 7.4. (2) The strength of ^{13}C NMR signals can be increased by a factor of up to 3, or the time required to reach a given signal to noise ratio can be cut by about a factor of 10 if one utilizes the nuclear

Overhauser enhancement (NOE) obtained through proton decoupling during carbon FID acquisition. Thus, the {1H}-^{13}C NOE must be measured in order to correct the ^{13}C signal integrals for the enhancement factors. For small molecules in solution the NOE is 2.998. We have measured the NOE for citrate and found it to be 3.0 ± 0.1, in agreement with expectations. (3) One must know the number of carbon nuclei which give rise to a given peak, and correct for this multiplicity. For the : citrate, δ = 45 ppm signal, 2 carbons contribute (C2 and C5). (4) Finally, the NMR signal is proportional to the number of nuclei within the detector coil, but the constant of proportionality is unknown. We can correct for this by measuring the NMR signal from a known number of nuclei by using an internal standard present in all of the sample acquisitions. A 1 mm capillary intensity and chemical shift standard containing 10 µl CrAcAc-doped-acetonitrile (δ = 5 and 121 ppm) was used (Fig. 3). The determined citrate amount was also normalized to a standard tissue weight (1.0 gram). Representative control and tumor ^{13}C NMR spectra are shown in Fig. 5 (below).

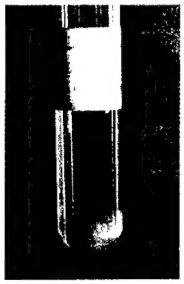

Figure 3. A human prostate tumor sample contained within a glass NMR tube. The black central rod is a fiber-optic thermometer probe for monitoring the sample temperature in real-time. The tumor sample is visible as the pink tissue at the bottom of the tube. The reference capillary containing 10 µl CrAcAc-doped-acetonitrile is visible to the left of the thermometer probe. The white plug at the top of the sample is teflon which serves to hold the thermometer and capillary in place during the measurement.

In order to calibrate the NMR measurements, the amount of citrate in a given tumor tissue sample was determined in two separate ways (1) by means of a citrate assay using a commercial product supplied by Boerhinger-Mannheim, and (2) by means of ^{13}C NMR spectroscopy combined with the above mentioned data correction factors. A correlation plot of the data obtained is shown as Fig. 4, where one notes that the NMR-determined citrate values agree with those found using the enzymatic assay. The slope of the least-squares line fitted to the data was 1.06 ± 0.10 (which is not significantly different from 1.0) with an r^2 = 0.91. The intercept was not significantly different from zero (-0.54 ± 0.76). These data indicate that all of the citrate in tumor tissue is visible to NMR and that the NMR method provides accurate quantitation of tumor metabolites.

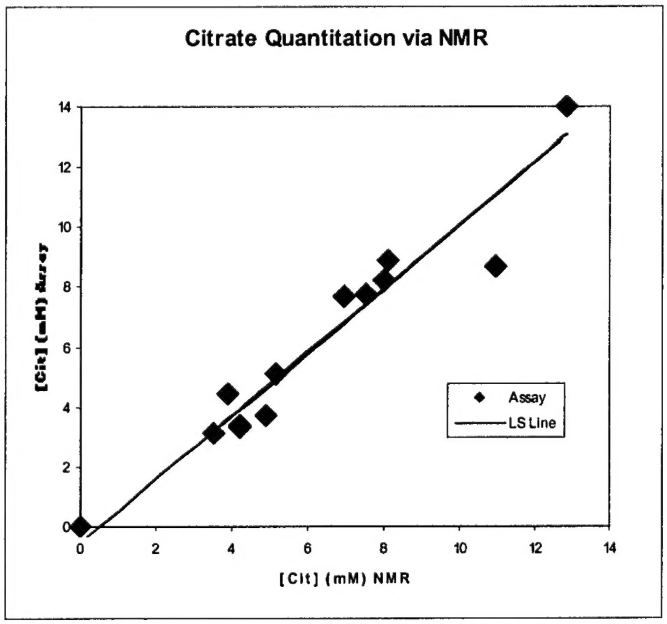

Figure 4. Relationship between prostate tissue citrate concentrations determined by means of an enzymatic citrate assay and ^{13}C NMR Spectroscopy. The line is a least-squares fit to the data with a slope of 1.06 ± 0.10 and r^2 = 0.91.

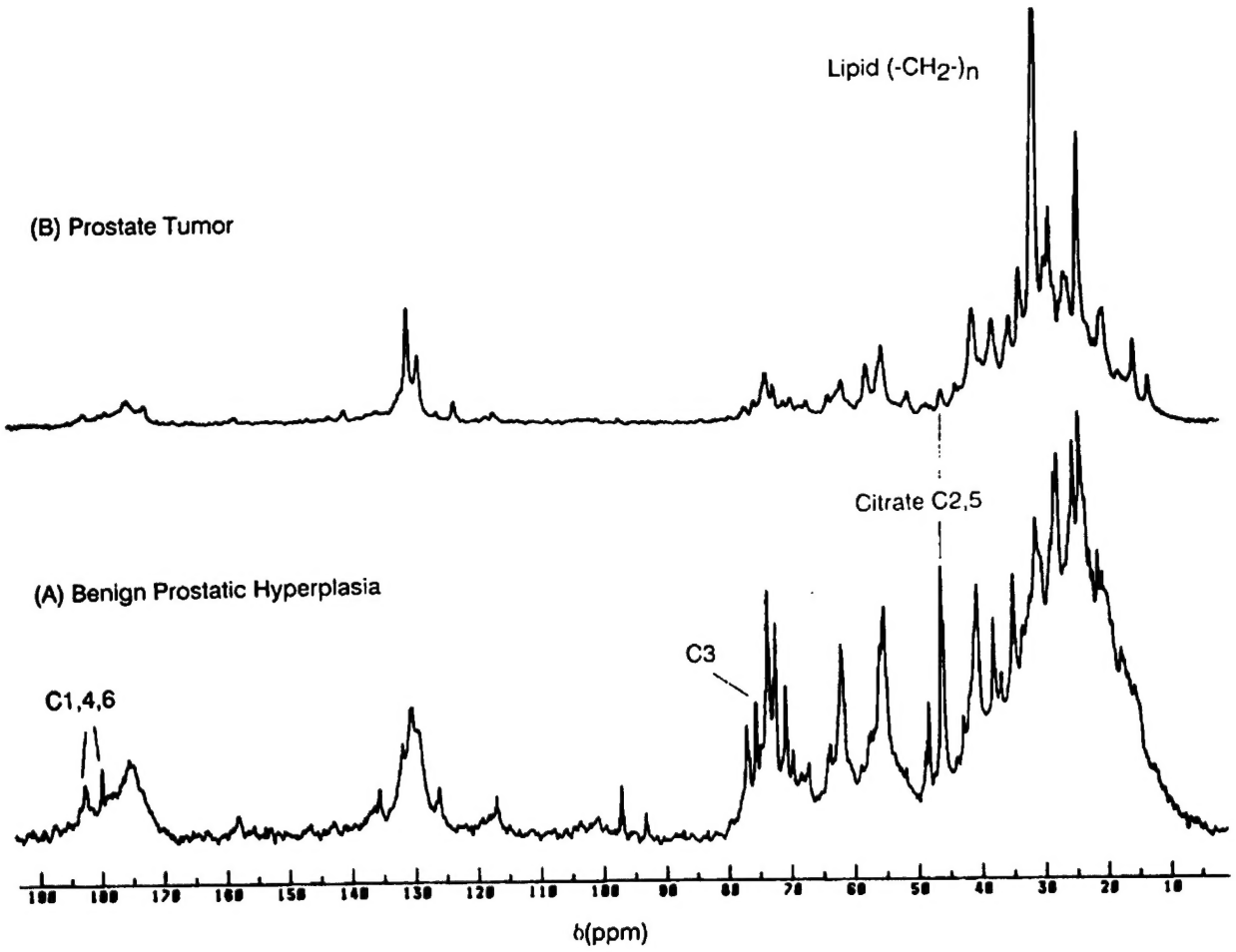

Figure 5. Natural abundance, proton-decoupled ^{13}C NMR spectra at 100.61 MHz of (A) non-malignant benign hyperplastic prostate tissue, and (B) prostate tumor tissue. Indicated are the resonances from citrate (C2,5; C3; and C1,4,6) and from the methylene $(-CH_2-)_n$ carbons. A 22.5 kHz sweep was accumulated in 16,384 data points in an acquisition time of 0.326 s following a 90° pulse. The pulse repetition rate was 0.94/sec. In order to minimize sample heating, a bilevel WALTZ-16 decoupling scheme was used with a power level of 1 Watt applied during the acquisition time and a level of 0.4 Watt applied during the interpulse delay.

^{13}C NMR of non-malignant human prostate tissue.

We next turned to the measurement of a number of metabolites in prostate tissue samples by means of ^{13}C NMR spectroscopy. The results (Fig. 5A) show that we can observe, natural-abundance ^{13}C NMR spectra from tissue samples obtained from residual human prostate tissue obtained during surgical resection of the gland. Signals from citrate carbons $C_{2,5}$ and lipid methylene carbons $(-CH_2-)_n$ were resolved well-enough so that measurements could be made of their respective intensities. Quantitative agreement was found between the citrate integrals (at δ = 47 ppm), relative to the standard, and the results of an enzymatic assay performed on the tissue after the NMR studies were completed (see above).

^{13}C NMR of malignant human prostate tissue.

A Natural-abundance ^{13}C NMR spectrum of a sample of human prostate tumor (Fig. 5B) shows that the citrate signal in the tumor is markedly smaller, while the lipid methylene signal (at 30.5 ppm, Fig. 3B) is much larger than that seen in the normal tissue. Other resonances areise from lactate (20.9 ppm) and inositol (near 74 ppm).

Citrate and lipids in nonmalignant vs malignant prostate.

The citrate $C_{2,5}$ (δ = 47 ppm) and lipid methylene $(-CH_2-)_n$ (δ = 30.5 ppm) carbon peak heights were measured and corrected for differences in sample weights, by normalization to the signal intensity per gram of tissue with respect to the intensity of the standard. The data were pooled into tumor (n=10) and non-malignant (n=24) groups based on the histologic diagnosis. Overall, the data (Fig. 6) confirmed that citrate amounts are higher and lipid amounts are lower in benign tissue in comparison to malignant tissue. The difference in normalized citrate peak intensity between benign and malignant human prostatic tissue was found to be statistically significant by Student's t-test for unequal variances ($p < 0.02$). There is overlap between the two groups, however, because citrate levels alone are unable to discriminate between low citrate tumors and low citrate stromal hyperplasia. Comparison of the lipid methylene peak intensities revealed that lipid differences between benign and malignant tissue values are even more significant ($p < 0.005$), and with less overlap.

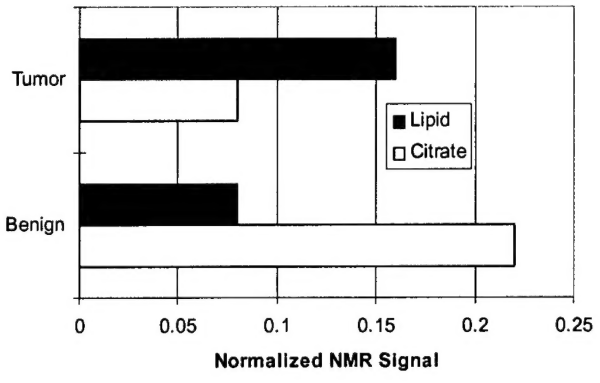

Figure 6. Citrate and lipid (triacylglycerol) results from ^{13}C NMR spectroscopy of 34 human prostate samples.

Correlation of citrate amounts with prostatic epithelial area.

The prostate is an exocrine gland which normally secretes a mixture of citrate and other compounds into seminal plasma. The secretory component of the tissue is presumably the epithelium which lines the acini. We sought to determine if histological data derived from our inital sample of tissues was congruent with our NMR results. We determined the amount of epithelium (expressed as a percentage of the total measured area) of our samples by using optical stereology of the stained tissue sections. The NMR results were obtained from the sample of 34 specimens mentioned above. The results showed that there was a direct correlation between the epithelial area and citrate production (Fig. 7) in the benign samples. The slope of the linear fit to the data is significantly different from zero ($p < 0.001$). It is interesting to note that the fitted line passes through the origin, implying that we were correct in our assumption that epithelium alone produces citrate. On the other hand, the results for the malignant samples (Fig. 7) show a weak inverse correlation between citrate and epithelial area. This is to be expected if our hypothesis about the lack of citrate production in tumors is correct. Note that the tumors have large areas of epithelium and low amounts of citrate. At high amounts of epithelium, most of the epithelial tissue is malignant. Presumably the citrate produced in tumors comes predominantly from the areas of nonmalignant epitheliun, and that is why the fitted line has a negative slope.

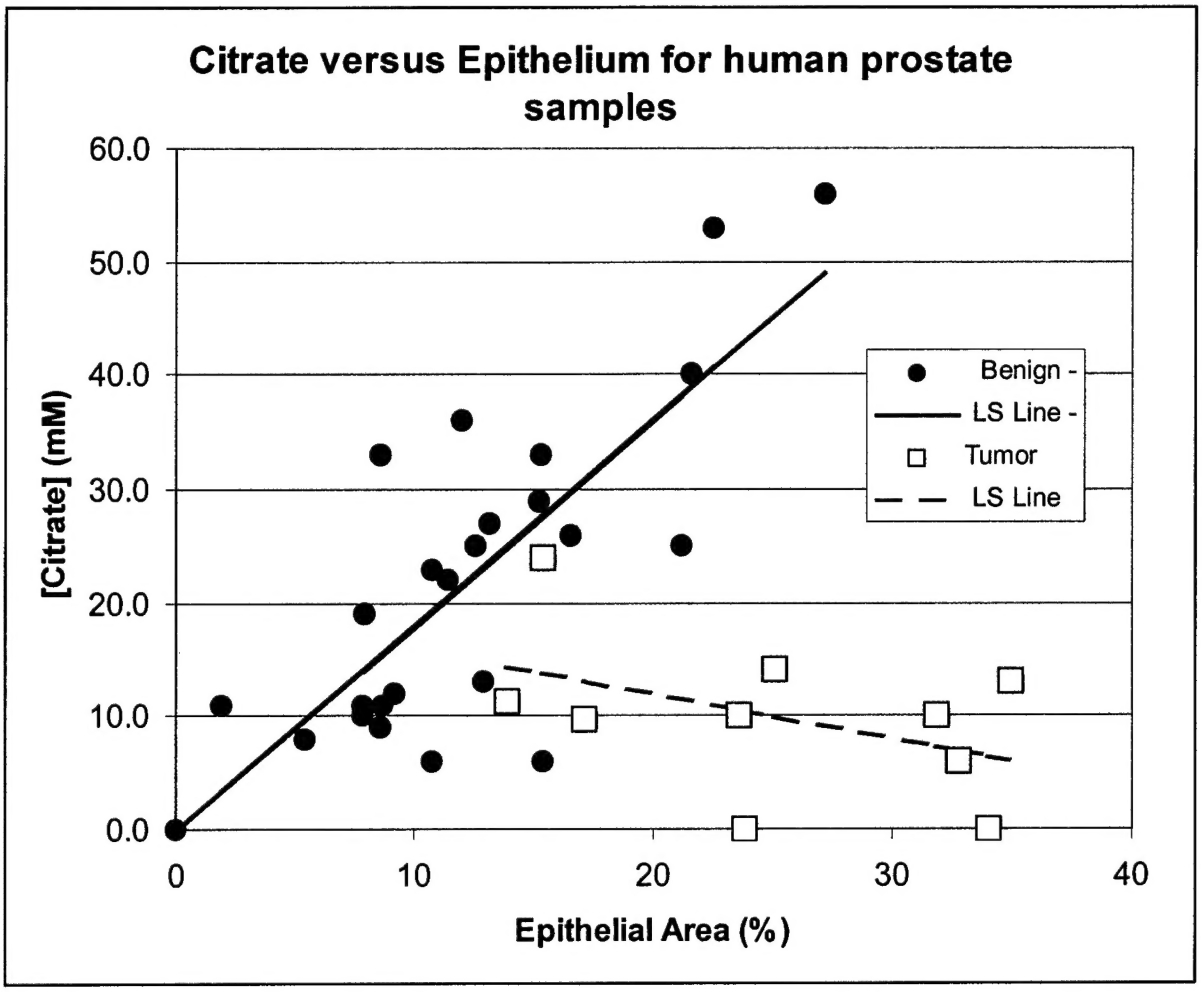

Figure 7. Relationship between the concentration of citrate determined by means of quantitative ^{13}C NMR spectroscopy and the amount of epthelium in H&E stained sections determined by area analysis of the same human prostatic adenocarcinoma tissues.

C. Computer-based Linear Discriminant Analysis.

In order to utilize all of the information present in a ^{13}C NMR spectrum of prostate tissue, we have been working on the development of machine-learning techniques which could be applied in a clinical setting to distinguish NMR spectra from malignant and non-malignant prostate tissue samples. Our first approach is to use Linear Discriminant Analysis (LDA) to develop an empirical discrimination function based on the following types of data, the local amounts of prostate specific metabolites determined by NMR, optical and video histology of the tissue sections, Gleason score, PSA, PAP and special stains measurements, and the patient's progress, to determine the best linear discriminant predictors of tumor diagnosis, grade, and hormonal sensitivity based on the measurements. Clearly progress along these lines requires an investment in both computer hardware and software. We have purchased the commercial SAS package because it contains LDA code which we can begin to use for our analysis. The SAS software now runs on a Sun-Blade 1000

with dual 750 MHz cpus and 16 gigabytes of RAM. We are currently working on algorithms which will automatically measure the ^{13}C NMR data and convert these measurements into a format compatible with SAS. Since this is a longer-term goal, we will report on our detailed progress in subsequent annual reports. Given the feedback from the LDA we will seek to refine our measurement of the predictors identified by the LDA in order to evaluate the potential for the developed empirical discrimination function for NMR to be used as a new diagnostic tool to predict tumor properties, with particular attention paid to androgen-sensitivity.

D. Application of non-invasive NMR spectroscopy in human patients.

^{1}H NMR Detection of citrate in prostatic tissue.

A representative high field (400 MHz) ^{1}H spectrum from benign human prostatic tissue (Fig. 8) shows the two doublets corresponding to citrate $H_{2,5}$ at δ = 2.6 ppm. Lactate appears at 1.3 ppm, and inositol appears at 3.6 ppm. The down-field region of the ^{1}H spectrum of this prostate tissue sample (not shown) displayed signals from aromatic protons, particularly from tyrosine at 6.9 and 7.2 ppm (*vide infra*) and phenylalanine. The metabolite lines in this spectrum are broadened by magnetic susceptibility variations from point to point within the tissue to a width of 23 Hz. These narrower resonances also ride on top of a broader baseline hump from the tissue and on the wings of the large residual water signal, even though the tissue sample was placed into a deuterated buffer, and the residual water signal was suppressed with gated proton decoupling. These results show that prostate metabolites, including citrate, are observable with proton NMR spectroscopy, in addition to that of ^{13}C NMR. Although we have applied ^{13}C NMR spectroscopy to human studies (Sillerud et al., 1988) we find that proton spectroscopy is technically less-demanding, and therefore more suited to initial clinical studies. We therefore turned to localized proton spectroscopy and imaging of the prostate in human cancer patients and in normal controls.

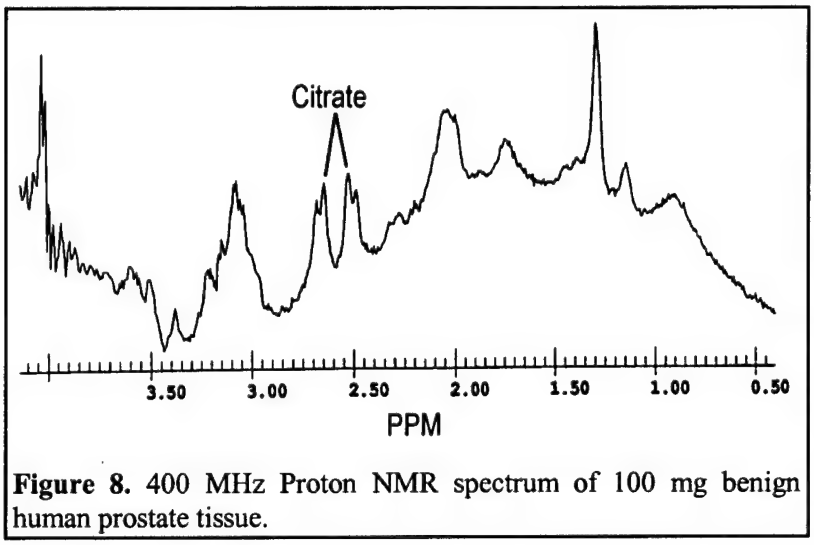

Figure 8. 400 MHz Proton NMR spectrum of 100 mg benign human prostate tissue.

NMR imaging of the prostate.

Proton NMR imaging and relaxation time measurements are able to provide important staging information relative to the extent of prostatic malignant disease, but are currently only able to differentiate between hyperplastic and malignant tissue on the basis of tissue contrast. No information is provided about the grade of the lesion. Prostate NMR imaging is generally well-established with several institutions using body-coil images and endorectal coils. Image-guided spectroscopy requires establishment of a high-quality image data set prior to the spectroscopic examination of the prostate. We have imaged several prostates of healthy male volunteers using a proton pelvic coil. We paid particular attention to how well the gland differs in contrast from surrounding tissue. Our results (using a T_2-weighted sequence [T_R=4 s, T_E=156 ms, 3 mm slice])

(Fig. 9) show both the central and the peripheral zones of the prostate. There is good discrimination of the gland from the surrounding tissue, and from the adjacent seminal vesicles. The images show that we should be able to perform a three-dimensional reconstruction of the prostate upon which we can then superimpose our chemical shift imaging results.

Figure 9. Proton NMR images of the male pelvis. The **left** image is an axial section through the prostate taken with T_R=4 sec, T_E = 156 ms, thus giving T_2 weighting. Note the good differentiation of the prostate anatomy into the central and peripheral zones. Most tumors occur in the peripheral zone. The image on the **right** is from a coronal section through the prostate taken with the same acquisition parameters.

Detection of Citrate in phantoms in the GE Whole Body NMR system.

We have taken single-pulse spectra, using a 30 cm diameter head coil (and with the 15 cm double-Helmholtz pelvic coil), of a phantom (0.75 M citrate in H_2O) on the GE 1.5 T NMR system. The signal to noise ratio for a single pulse was found to be 72 ± 6 for the 4 methylene ($-CH_2-$) protons of citrate. The total line width for the citrate methylene protons was 6.9 Hz, and the width of the water signal was 4.3 Hz. These results are indicative of the expected sensitivity and resolution to be obtained *in vivo*, and reflect the excellent progress that we have made shimming this system. These results are also typical of what other workers in the field have obtained using similar phantoms, and in patients. We expect to obtain linewidths around 5-10 Hz in patients.

In vivo ^{1}H detection of human prostatic citrate.

We have used both a proton pelvic coil and an endorectal coil (Medrad, Inc.) to detect prostatic metabolites *in vivo* in healthy male volunteers using the STEAM protocol. Fig. 10 shows the placement of the STEAM voxel onto the NMR image from a normal male volunteer. The volume of the voxel was 8 ml, and this encompassed both the central and the peripheral zones of the gland. We were able to place this voxel well away from the rectum, the bladder, and from periprostatic fat, which could interfere with lipid measurements.

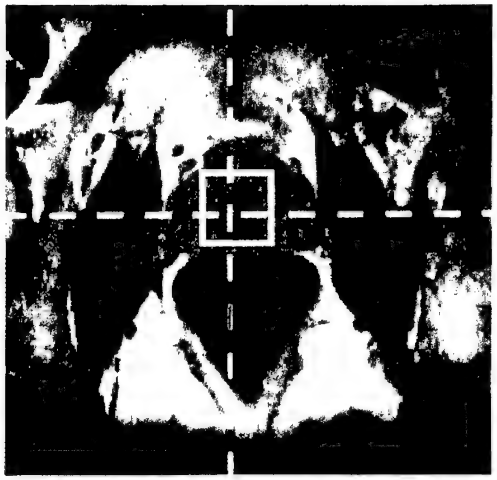

Figure 11. Placement of a STEAM voxel region of interest onto the prostate image of a normal male volunteer in order to obtain localized proton NMR spectra from this volume.

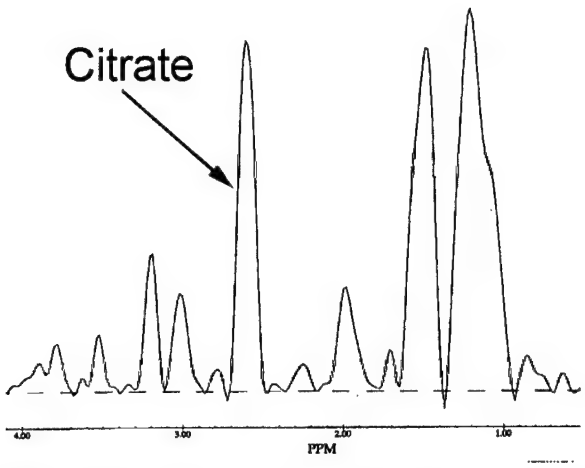

Figure 12. STEAM localized proton NMR spectrum at 1.5 Tesla of the prostate from a normal male volunteer. The citrate resonance is indicated at δ = 2.6 ppm.

The results from one such NMR spectroscopic exam (Fig. 12) show a signal at the characteristic chemical shift of citrate (δ = 2.6 ppm). Note that citrate resonates in a region of the spectrum which is relatively free from interference from other resonances. We also can observe nuclear resonances from choline (δ = 3.2 ppm), creatine (δ = 3.0 ppm), and glutamate (δ = 2.0 ppm). We anticipate the acquisition of even better proton spectra from humans *in vivo* as the localized spectroscopy program proceeds. The width of the citrate signal is 6.9 Hz, in agreement with our expectations (*vide supra*).

Key Research Accomplishments

1. The normal prostate contains modest amounts of epithelium; the average is 12.7 ± 5.9 % by area. Prostatic adenocarcinoma, on the other hand contains twice the epithelium at 25.3 ± 7.9 % by area.

2. All of the citrate in prostatic tissue is visible to NMR.

3. The NMR method provides accurate quantitation of tumor metabolites.

4. We can observe, natural-abundance ^{13}C NMR spectra from tissue samples obtained from residual human prostate tissue obtained during surgical resection of the gland. Signals from citrate carbons $C_{2,5}$ and lipid methylene carbons $(-CH_2-)_n$ were resolved well-enough so that measurements could be made of their respective intensities. Quantitative agreement was found between the citrate integrals (at δ = 47 ppm), relative to the standard, and the results of an enzymatic assay performed on the tissue after the NMR studies were completed.

5. Citrate amounts are higher and lipid amounts are lower in benign tissue in comparison to malignant tissue. The difference in normalized citrate peak intensity between benign and malignant human prostatic tissue was found to be statistically significant by Student's t-test for unequal variances ($p < 0.02$).

6. Comparison of the lipid methylene peak intensities from ^{13}C NMR spectra of human prostate tissue revealed that lipid differences between benign and malignant tissue values are even more significant ($p < 0.005$), and with less overlap, than the citrate differences.

7. There is a direct correlation between prostate epithelial area and citrate production in the benign samples. The slope of the linear fit to the data is significantly different from zero ($p < 0.001$). The results for the malignant prostate tumor samples show a weak inverse correlation between citrate and epithelial area.

8. High field (400 MHz) ^1H spectra from benign human prostatic tissue show signals from citrate $H_{2,5}$ at δ = 2.6 ppm. Lactate appears at 1.3 ppm, and inositol appears at 3.6 ppm. The down-field region of the ^1H spectrum of this prostate tissue sample displayed signals from aromatic protons, particularly from tyrosine at δ = 6.9 and 7.2 ppm and phenylalanine.

9. Prostate NMR imaging (using a T_2-weighted sequence [T_R=4 s, T_E=156 ms, 3 mm slice]) shows both the central and the peripheral zones of the prostate.

10. We have used both a proton pelvic coil and an endorectal coil (Medrad, Inc.) to detect prostatic metabolites *in vivo* in healthy male volunteers using the STEAM protocol. An NMR spectroscopic exam shows signals at the characteristic chemical shift of citrate (δ = 2.6 ppm) as well as choline (δ = 3.2 ppm), creatine (δ = 3.0 ppm), and glutamate (δ = 2.0 ppm).

Reportable outcomes

1. The normal prostate contains modest amounts of epithelium; the average is 12.7 ± 5.9 % by area. Prostatic adenocarcinoma, on the other hand contains twice the epithelium at 25.3 ± 7.9 % by area.

2. All of the citrate in prostatic tissue is visible to NMR.

3. The NMR method provides accurate quantitation of tumor metabolites.

4. We can observe, natural-abundance ^{13}C NMR spectra from tissue samples obtained from residual human prostate tissue obtained during surgical resection of the gland. Signals from citrate carbons $C_{2,5}$ and lipid methylene carbons $(-CH_2-)_n$ were resolved well-enough so that measurements could be made of their respective intensities. Quantitative agreement was found between the citrate integrals (at δ = 47 ppm), relative to the standard, and the results of an enzymatic assay performed on the tissue after the NMR studies were completed.

5. Citrate amounts are higher and lipid amounts are lower in benign tissue in comparison to malignant tissue. The difference in normalized citrate peak intensity between benign and malignant human prostatic tissue was found to be statistically significant by Student's t-test for unequal variances ($p < 0.02$).

6. Comparison of the lipid methylene peak intensities from ^{13}C NMR spectra of human prostate tissue revealed that lipid differences between benign and malignant tissue values are even more significant ($p < 0.005$), and with less overlap, than the citrate differences.

7. There is a direct correlation between prostate epithelial area and citrate production in the benign samples. The slope of the linear fit to the data is significantly different from zero ($p < 0.001$). The results for the malignant prostate tumor samples show a weak inverse correlation between citrate and epithelial area.

Conclusions

The normal prostate contains modest amounts of epithelium; the average is 12.7 ± 5.9 % by area. Prostatic adenocarcinoma, on the other hand contains twice the epithelium at 25.3 ± 7.9 % by area. All of the citrate in prostatic tissue is visible to NMR. The NMR method provides accurate quantitation of tumor metabolites. We can observe, natural-abundance ^{13}C NMR spectra from tissue samples obtained from residual human prostate tissue obtained during surgical resection of the gland. Signals from citrate carbons $C_{2,5}$ and lipid methylene carbons $(-CH_2-)_n$ were resolved well-enough so that measurements could be made of their respective intensities. Quantitative agreement was found between the citrate integrals (at δ = 47 ppm), relative to the standard, and the results of an enzymatic assay performed on the tissue after the NMR studies were completed. Citrate amounts are higher and lipid amounts are lower in benign tissue in comparison to malignant tissue. The difference in normalized citrate peak intensity between benign and malignant human prostatic tissue was found to be statistically significant by Student's t-test for unequal variances ($p < 0.02$). Comparison of the lipid methylene peak intensities from ^{13}C NMR spectra of human prostate tissue revealed that lipid differences between benign and malignant tissue values are even more significant ($p < 0.005$), and with less overlap, than the citrate differences. There is a direct correlation between prostate epithelial area and citrate production in the benign samples. The slope of the linear fit to the data is significantly different from zero ($p < 0.001$). The results for the malignant prostate tumor samples show a weak inverse correlation between citrate and epithelial area. High field (400 MHz) ^1H spectra from benign human prostatic tissue show signals from citrate $H_{2,5}$ at δ = 2.6 ppm. Lactate appears at 1.3 ppm, and inositol appears at 3.6 ppm. The down-field region of the ^1H spectrum of this prostate tissue sample displayed signals from aromatic protons, particularly from tyrosine at δ = 6.9 and 7.2 ppm and phenylalanine. Prostate NMR imaging (using a T_2-weighted sequence [T_R=4 s, T_E=156 ms, 3 mm slice]) shows both the central and the peripheral zones of the prostate. We have used both a proton pelvic coil and an endorectal coil (Medrad, Inc.) to detect prostatic metabolites *in vivo* in healthy male volunteers using the STEAM protocol. An NMR spectroscopic exam shows signals at the characteristic chemical shift of citrate (δ = 2.6 ppm) as well as choline (δ = 3.2 ppm), creatine (δ = 3.0 ppm), and glutamate (δ = 2.0 ppm). These results indicate that we have made significant progress with respect to our specific aims during the initial funding year of this project. We are now in a good position to pursue computer-fitting of the NMR spectra with the aim to incorporate this data into an LDA scheme for the determination of the most significant metabolic differences between normal and malignant prostates. Our in vivo program of application of this research to human patients is now on a firm foundation. We look forward to the next year of research with eager anticipation because we are replacing our aging GE 1.5 Tesla whole body NMR system with a state-of-the-art Seimens instrument. This new instrument will be able to acquire chemical shift images of metabolites in the prostate with superior resolution and sensitivity.

References

Sillerud LO, Halliday KR, Griffey RH, et al: (1988) In vivo ^{13}C spectroscopy of the human prostate. Magn. Reson. Med. **8**:224-230.

Appendices: none